Heliyon 10 (2024) e28490

Contents lists available at ScienceDirect

Heliyon

journal homepage: www.cell.com/heliyon

Research article

Integrated analysis of scRNA-seq and bulk RNA-seq identifies *FBXO2* as a candidate biomarker associated with chemoresistance in HGSOC

Wenwen Lai [a,b,c,1], Ruixiang Xie [d,1], Chen Chen [e], Weiming Lou [f], Haiyan Yang [b,c], Libin Deng [b,c], Quqin Lu [b,c], Xiaoli Tang [e,*]

[a] *Department of Organ Transplantation, The Second Affiliated Hospital of Nanchang University, Nanchang, Jiangxi, China*
[b] *Jiangxi Provincial Key Laboratory of Preventive Medicine, Nanchang University, Nanchang, Jiangxi, China*
[c] *Department of Biostatistics and Epidemiology, School of Public Health, Nanchang University, Nanchang, Jiangxi, China*
[d] *School of Life Science, Nanchang University, Nanchang University, Nanchang, China*
[e] *College of Basic Medical Science, Nanchang University, Nanchang, China*
[f] *Academic Affairs Office, The Second Affiliated Hospital of Nanchang University, Nanchang, Jiangxi, China*

ARTICLE INFO

Keywords:
High-grade serous ovarian carcinoma
Chemoresistance
Biomarker
Single-cell RNA-seq
Bulk RNA-seq

ABSTRACT

Background: High-grade serous ovarian carcinoma (HGSOC) is the most prevalent and aggressive histological subtype of epithelial ovarian cancer. Around 80% of individuals will experience a recurrence within five years because of resistance to chemotherapy, despite initially responding well to platinum-based treatment. Biomarkers associated with chemoresistance are desperately needed in clinical practice.

Methods: We jointly analyzed the transcriptomic profiles of single-cell and bulk datasets of HGSOC to identify cell types associated with chemoresistance. Copy number variation (CNV) inference was performed to identify malignant cells. We subsequently analyzed the expression of candidate biomarkers and their relationship with patients' prognosis. The enrichment analysis and potential biological function of candidate biomarkers were explored. Then, we validated the candidate biomarker using *in vitro* experiments.

Results: We identified 8871 malignant epithelial cells in a single-cell RNA sequencing dataset, of which 861 cells were associated with chemoresistance. Among these malignant epithelial cells, *FBXO2* (F-box protein 2) is highly expressed in cells related to chemoresistance. Moreover, *FBXO2* expression was found to be higher in epithelial cells from chemoresistance samples compared to those from chemosensitivity samples in a separate single-cell RNA sequencing dataset. Patients exhibiting elevated levels of *FBXO2* experienced poorer outcomes in terms of both overall survival (OS) and progression-free survival (PFS). *FBXO2* could impact chemoresistance by influencing the PI3K-Akt signaling pathway, focal adhesion, and ECM-receptor interactions and regulating tumorigenesis. The 50% maximum inhibitory concentration (IC50) of cisplatin decreased in A2780 and SKOV3 ovarian carcinoma cell lines with silenced *FBXO2* during an *in vitro* experiment.

Conclusions: We determined that *FBXO2* is a potential biomarker linked to chemoresistance in HGSOC by combining single-cell RNA-seq and bulk RNA-seq dataset. Our results suggest that

* Corresponding author.
E-mail address: xltangmail@163.com (X. Tang).
[1] These authors contributed equally to this work.

https://doi.org/10.1016/j.heliyon.2024.e28490
Received 19 November 2023; Received in revised form 19 March 2024; Accepted 20 March 2024
Available online 25 March 2024

FBXO2 could serve as a valuable prognostic marker and potential target for drug development in HGSOC.

1. Background

Epithelial ovarian cancer (EOC) is a deadly cancer that ranks eighth in causing cancer-related deaths globally, with around 207,252 fatalities reported in 2020 [1]. High-grade serous ovarian carcinoma (HGSOC) is the predominant and most aggressive type, making up around 75% of all EOCs [2]. Due to inadequate screening methods, approximately 80% of patients receive a diagnosis in later stages, leading to unfavorable survival rates [3]. The 5 year cause specific survival rates for stage III and stage IV HGSOC patients are only 42% and 26%, respectively [3]. Surgical debulking followed by platinum-based chemotherapy is currently the primary treatment option for patients with HGSOC [4]. Regrettably, around 80% of individuals will experience a recurrence within five years because of chemoresistance, despite the fact that the majority of patients initially exhibit a positive reaction to platinum-based chemotherapy [5,6]. Extensive efforts have been made to overcome this pervasive problem, but chemoresistance in HGSOC is still an unsolved challenge.

An increasing number of studies have focused on overcoming the chemoresistance of HGSOC throughout the past few years with high-throughput sequencing technology. Koti M et al. discovered a group of genes that play a role in the insulin like growth factor 1/PI3K/nuclear factor kappa-B/extracellular regulated protein kinases signaling pathways, impacting the response to chemotherapy through bulk RNA sequencing (RNA-seq) [7]. Paola et al. reported that the microRNA 23a-3p/apoptotic peptidase activating factor 1 axis may be a possible target to overcome platinum resistance [8]. However, the composition of the cell type in bulk tissues remains unclear. Liu et al. found that there exists a unique tumor microenvironment in HGSOC [9] and it has been proven to exert an important influence on chemoresistance and prognosis of HGSOC patients [10–12]. However, the tumor microenvironment is masked due to the drawback of bulk RNA-seq, which makes it impossible to understand the change in cell components and cell crosstalk during HGSOC chemoresistance.

Lately, there has been a growing interest in using single-cell RNA sequencing (scRNA-seq) to investigate the chemoresistance of HGSOC. It has the ability to capture gene expression at the level of individual cells and distinguish between different types of cells. Research has uncovered the single-cell landscape of HGSOC and its diversity with the tumor microenvironment through scRNA-seq, offering important information for discovering novel molecular pathways and possible targets for chemoresistance [13–15]. On the other hand, Zhang et al. examined the transcriptomic data of individual cells from HGSOC patients both pre- and post-chemotherapy, revealing a steady rise in stress-related cell activity throughout the treatment process [16]. Furthermore, Hao et al. reported that a subset of epithelial cells may enhance proliferative potential and chemoresistance in HGSOC [17].

Researchers prefer the combined examination of single-cell RNA-seq and bulk RNA-seq as it allows them to leverage the strengths of each method. Previous research has shown the diversity of immune cells and created a predictive pattern in ovarian cancer using this method [18,19]. More than that, Wang et al. reported patients with ovarian cancer who were to be in the high-risk category showed reduced sensitivity to chemotherapy medications [20]. Herein, we aimed to identify the biomarker associated with chemoresistance that could provide guidance for clinical treatment by comprehensively analyzing the transcriptomic profiles of bulk RNA-seq datasets and scRNA-seq datasets from HGSOC samples.

2. Materials and methods

2.1. Acquisition of datasets

Data on gene expression matrix and clinical information for patients with HGSOC were acquired from The Cancer Genome Atlas-ovarian serous cystadenocarcinoma (TCGA-OV) dataset. We performed data clean-up. Patient cases without a platinum-free interval (PFI) were excluded, along with those lacking RNA-seq data despite having a PFI. In addition, based on their PFI, HGSOC patients were divided into chemoresistance samples (PFI $<$6 months) and chemosensitivity samples (PFI $\geq$6 months) [21]. Finally, 188 HGSOC patients with PFI information and corresponding RNA-seq data were enrolled in this study, including 128 chemosensitivity patients and 60 chemoresistance patients.

The two HGSOC scRNA-seq datasets were obtained from the Gene Expression Omnibus (GEO) database. The GSE158937 dataset consisted of three HGSOC samples collected before underwent therapy from high-grade serous ovarian primary tumors [22,23]. The GSE154600 dataset consisted of five human HGSOC samples collected after underwent therapy from the omentum metastasis of high-grade serous ovarian tumors [24]. Of these five samples, one sample had a chemotherapy response that was neither

Table 1
The key characteristics of the datasets in this study.

Datasets	Type	Chemoresistance	Chemosensitivity
TCGA-OV	Tissue	60	128
GSE158937	Tissue	3	0
GSE154600	Tissue	2	2
GSE47856	Cell line	–	–

chemoresistance nor chemosensitivity, so we excluded it. Therefore, two chemoresistance samples and two chemosensitivity samples were included in our study. Furthermore, the genetic expression patterns of the A2780, OVCA429 and IGROV-1 human ovarian cancer cell lines in the GSE47856 dataset in the GEO repository were obtained [25]. Table 1 displayed the main features of the datasets analyzed in this research.

2.2. Processing of single-cell RNA-seq datasets

The scRNA-seq dataset was analyzed using Seurat in R 4.1.0 for quality control, statistical analysis, and exploration [26]. Data was processed based on specific quality control standards: 1) cells were screened for at least 100 genes detected, with genes expressed in less than 3 cells being excluded; 2) cells with nuclear gene counts below 200 or above 6000 and at least 50% mitochondrial genes were eliminated.

The analysis involved identifying the most variable genes using the FindVariableGenes method, followed by dimensionality reduction through principal component analysis (PCA) [27]. Clusters were identified by applying the FindClusters function with a resolution of 0.8, using the 20 principal components (PCs) as input. The selection of PCs was based on visualizing the decrease in PC variance explained with the ElbowPlot function. Next, the RuntSNE function was used to create t-distributed stochastic neighbor embedding (t-SNE) visualizations [28].

Using the FindMarkers function, marker genes were identified in each cluster based on the criteria of $\log_2$ [fold change (FC)] > 0.5 and an adjusted P value < 0.05. The 'SingleR' package was used to annotate clusters using the marker gene [29].

Then, the GSE154600 dataset was analyzed as described before. However, cells were excluded if their nuclei gene counts below 200 or above 5000, and if they had more than 25% mitochondria-expressed genes, as most cells in the dataset fell within these thresholds. Clusters were identified using the FindClusters function with resolution 0.8 with the 25 principal components were used as input, based on the assumption that the standard deviation remains relatively constant with 25 PCs.

2.3. Copy number variation inference

The estimation of large-scale chromosomal copy number variation (CNV) in somatic cells was performed using the "infercnv" R package [30]. Preparation of a raw count matrix for scRNA-seq, annotation files and gene/chromosome position files were done based on the data requirements (https://github.com/broadinstitute/inferCNV). We selected macrophages, monocytes, NK cells, T cells and B cells as reference normal cells. The CNV score was calculated as the quadratic sum of the CNV regions.

2.4. Identification of cells associated with chemoresistance

The "Scissor" R package was used to identify individual cells within subgroups that are correlated with chemoresistance [31]. Scissor requires a single-cell expression matrix, a bulk expression matrix and a phenotype of interest as inputs. Our research utilized the single-cell expression matrix obtained from GSE158937, along with the bulk expression matrix and associated PFI data from patients with HGSOC as the designated inputs.

2.5. Enrichment analysis of Kyoto Encyclopedia of Genes and Genomes pathways

Based on whether the cells were associated with chemoresistance, differentially expressed genes (DEGs) in malignant epithelial cells of the GSE158937 dataset were identified by the FindMarkers function in Seurat. A gene at $\log_2$FC greater than 0.5 and an adjusted P value less than 0.05 was considered a DEG. In the GSE154600 dataset, DEGs in epithelial cells of different origin samples were obtained in the same way. We analyzed the possible biological effects of DEGs by conducting Kyoto Encyclopedia of Genes and Genomes (KEGG) pathway using the "Clusterprofiler" R package [32]. A gene set at P less than 0.05 and false discovery rate less than 0.05 was deemed to be significantly enriched.

2.6. Identification of candidate biomarkers

Candidate biomarkers linked to chemoresistance were identified by comparing the DEGs between chemoresistance patients and chemosensitivity patients in the TCGA-OV dataset were identified using the "limma" R package [33]. A gene was considered a DEG if it had an adjusted P value of less than 0.05. Then, we had an intersection of three DEGs. The expression of overlapping genes between tumor samples and normal samples was explored by GEPIA2 (http://gepia2.cancer-pku.cn/). Furthermore, we categorized HGSOC individuals into two cohorts based on the median expression level of overlapping genes and plotted a Kaplan–Meier graph. Endpoints included both overall survival (OS) and progression-free survival (PFS). The prognostic value of shared genes for high-grade serous ovarian cancer was assessed with KM plotter (http://kmplot.com/analysis). Candidate biomarkers were identified as genes that exhibited high expression levels in the tumor samples and were linked to unfavorable prognosis.

2.7. Protein–protein interaction network of candidate biomarkers and enrichment analysis

In order to investigate the functional significance of the potential biomarker, we gathered genes that interact with it from three protein–protein interaction (PPI) network databases: STRING [34], BioGRID [35] and HPRD [36]. Furthermore, we gathered the

roster of genes associated with ovarian cancer from the CTD database [37] and the roster of immune-related genes from the IMPORT database [38]. We defined the candidate biomarker as node1 and other genes interacting with it as node2, then we visualized the gene interaction network by Cytoscape [39]. Additionally, the genes were subjected to GO analysis and KEGG pathway analysis using the "Clusterprofiler" R package to investigate the roles of this interaction network module dominated by the potential biomarker.

2.8. Exploration of the relationship between the candidate biomarker and tumor stemness in HGSOC

In order to investigate the connection between the potential biomarker and tumor stemness in HGSOC, we initially examined the expression of candidate biomarker in different cell types within the GSE158937 dataset. Based on the median expression level of the candidate biomarker, the epithelial cells were categorized into a high expression group and a low expression group. Then we conducted differentially expressed analysis for epithelial cells in these two groups. Furthermore, the DEGs were subjected to KEGG pathway analysis and GO analysis using the "Clusterprofiler" R package. Gene set enrichment analysis (GSEA) was conducted with GSEA software, utilizing hallmark pathways gene sets obtained from the Molecular Signatures Database (http://www.gsea-msigdb.org/gsea/msigdb/index.jsp). A false discovery rate of less than 0.05 and a *P* value of less than 0.05 were considered the threshold for significance. Through reviewing the relevant literature, we obtained the marker gene of cancer stem-like cells in HGSOC and conducted correlation analysis for the marker gene and the candidate biomarker in the epithelial cells of high expression group.

2.9. Cell culture, transfection and chemosensitivity assay

The A2780 and SKOV3 ovarian carcinoma cell lines were acquired from the American Type Culture Collection (Manassas, VA, USA) and the Chinese Academy of Sciences Cell Bank (Beijing, China). Cells were grown in 1640 medium with 10% fetal bovine serum in a humid incubator at 37 °C and 5% CO2, supplemented for the A2780 cell line or Dulbecco's modified Eagle's medium for the SKOV3 cell line. The cells were placed in a 6-well plate and grown until they reached 50% confluenc. Cells were transiently transfected using SiTran 2.0 following the instructions provided by the manufacturer. The sequence of the siRNA was shown in Table 2. And the knockdown of the transcript was confirmed by Western blot experiment. The culture medium was changed after 24 h, and the cells were then cultured for another 24 h.

96-well plates were filled with cells (10,000 cells per well) and exposed to varying concentrations of cisplatin in triplicate, ranging from 0 to 12 μg/ml. Cell viability was assessed using a CCK-8 assay after 48 h, with the optical density measured at 450 nm by an automated microplate reader. The 50% maximum inhibitory concentration (IC50), representing the concentration at which cell growth decreased by half compared to control cell growth, was determined using GraphPad Prism 5.0 software (GraphPad, Inc., San Diego, CA, USA).

3. Results

3.1. Malignant epithelial cells predominate in HGSOC

The GSE158937 dataset contained a sum of 15,192 cells. Following quality control (Fig S1A-S1E), a total of 11,300 cells were retained for additional examination. Afterwards, we effectively categorized the cells into 20 distinct clusters (Fig. 1A). A combined 14,463 marker genes were discovered across 20 clusters, with the heatmap showcasing the top 10 marker genes from each cluster (Fig. 1B–Table S1). In Fig. 1C, we identified that Clusters 0, 1, 2, 3, 4, 5, 7, 8, 9, 12 and 17, totaling 9206 cells, were epithelial cells; Clusters 6 and 18, totaling 735 cells, were macrophages; Clusters 11 and 16, totaling 443 cells, were fibroblasts; Cluster 10, totaling 397 cells, was T cells; Cluster 13, totaling 278 cells, was endothelial cells; Cluster 14, totaling 138 cells, was monocytes; Cluster 15, containing 61 cells, was NK cells; and Cluster 19, totaling 42 cells, was B cells. In Fig. 1D, the figure displays the quantities of different cell types, with epithelial cells being the most abundant. In addition, the CNV inference results showed that almost all epithelial cells had abnormal CNV levels and higher CNV scores than reference cells, which confirmed that epithelial cells were malignant cells (Fig. 1E–F).

3.2. Most cells associated with chemoresistance are malignant epithelial cells

In the GSE158937 dataset, 1401 cells associated with chemoresistance were identified (Fig. 2A), consisting of 861 epithelial cells, 265 macrophages, 161 fibroblasts, 67 T cells, 20 monocytes, 17 endothelial cells, 9 NK cells, and 1 B cell (Fig. 2B). Among 861 epithelial cells associated with chemoresistance and 8345 epithelial cells not associated with chemoresistance in the GSE158937 dataset, 164 DEGs were identified, including 125 upregulated genes and 39 downregulated genes (Fig. 2C). The analysis of these DEGs

Table 2
The sequence of the siRNA in the study.

Number	Sequence
stB0001215A	CACTGGCAGCAGTTCTACT
stB0001215B	ACGAGCTCACCGTTAAGCT
stB0001215C	GATGAGAGCGTCAAGAAGT

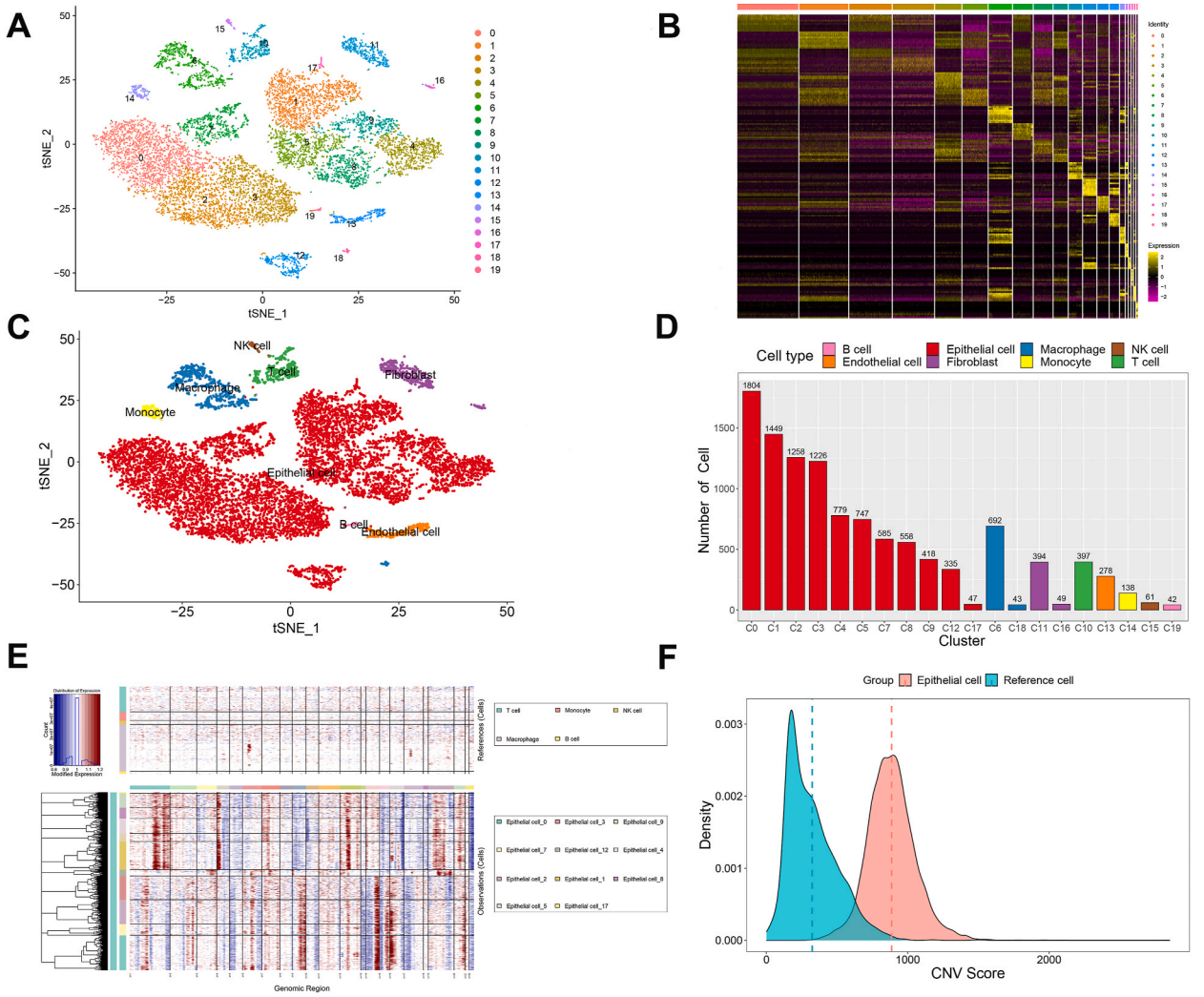

Fig. 1. Cell annotation and identification of malignant cells in the GSE158937 dataset. (A) 11,300 cells were divided into 20 separate clusters with resolution 0.8. (B) Heatmap displaying the top 10 marker genes in each cluster. (C) The t-SNE plot demonstrated cell types. (D) Cell number of each cluster. (E) Heatmap showing large-scale CNV profile of each cluster of epithelial cells and reference cell subpopulation; the red and blue colors represented high and low CNV level, respectively. (F) The distribution of CNV score for epithelial cell and reference cell and the dashed line represents the mean of CNV score.

using KEGG indicated that they were mainly enriched in ribosome, protein processing in endoplasmic reticulum, and chemical carcinogenesis – reactive oxygen species (Fig. 2D).

3.3. *Epithelial cells are involved in chemoresistance*

A total of 35,442 cells from the GSE154600 dataset were included in our study, which consisted of 24,416 cells from chemoresistance samples and 11,026 cells from chemosensitivity samples. A total of 33,054 cells were screened for subsequent analysis after quality control (Fig S2A-S2E). We divided the cells into 30 separate clusters (Fig S2F) and identified 6748 marker genes from all 30 clusters. The heatmap displayed the top 10 marker genes from every cluster (Fig S2G,Table S2). Clusters 2, 3, 8, 9, 10, 22 and 23, containing 10,003 cells, were epithelial cells.

All the cells in the chemoresistance samples and chemosensitivity samples are separately shown in Fig. 3A. There were 8259 epithelial cells from chemoresistance samples and 1744 epithelial cells from chemosensitivity samples in the GSE154600 dataset. A total of 799 DEGs were identified among these cells, including 445 upregulated genes and 354 downregulated genes (Fig. 3B). Notably, all the pathways related to chemoresistance identified in the GSE158937 dataset were contained in the results of KEGG analysis for these DEGs, which validated that epithelial cells were involved in HGSOC chemoresistance (Fig. 3C).

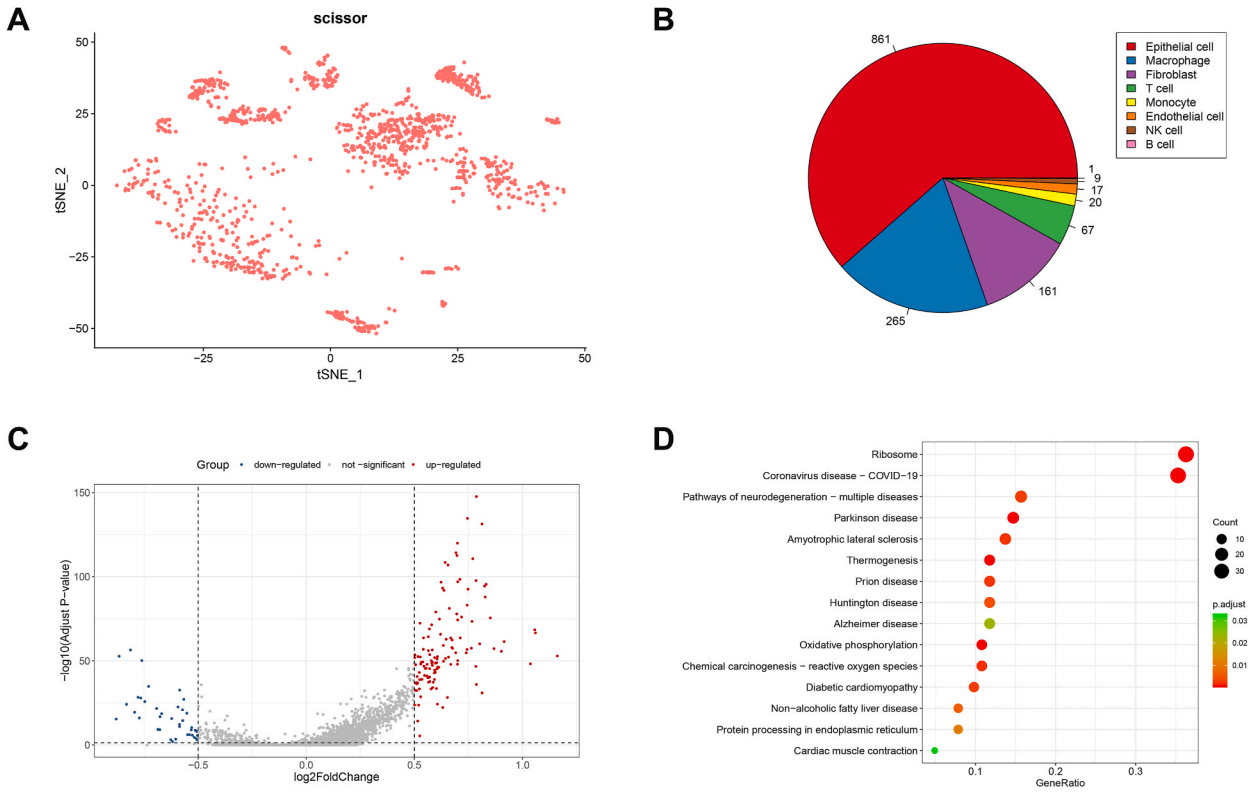

Fig. 2. Identification of cells associated with chemoresistance in the GSE158937 dataset and KEGG analysis. (A) The t-SNE visualization of the Scissor algorithm selected cells associated with chemoresistance. (B) The distribution of cells associated with chemoresistance in each cell type. (C) The differentially expressed genes (DEGs) between malignant epithelial cells associated with chemoresistance and those not associated with chemoresistance. (D) KEGG analysis of DEGs.

3.4. FBXO2 is identified as a candidate biomarker

Among these chemoresistance patients and chemosensitivity patients in the TCGA-OV dataset, 1805 DEGs were identified, including 312 upregulated genes and 1493 downregulated genes. Following the comparison of three sets of DEGs, *FBXO2*, *RPL6*, *RPL9*, *RPL10*, *RPL32*, *RGS10*, and *RPS23* were determined to be common genes (Fig. 3D). Fig. 4A–B displays the gene expression profiles in chemoresistance samples and chemosensitivity samples for the GSE154600 dataset and TCGA-OV dataset. Interestingly, *RPL9* and *RPS23* showed high expression levels in the normal samples, while *FBXO2* and *RGS10* exhibited high expression levels in the tumor samples (Fig. 4C, Fig S3A). Furthermore, individuals with elevated levels of *FBXO2* showed poorer OS and PFS compared to others (Fig. 4D–E, Fig S3B-3C). Taken together, these results identified *FBXO2* as a candidate biomarker associated with chemoresistance.

3.5. PPI network of FBXO2 and enrichment analysis

By integrating three protein–protein interaction network databases, 405 genes were confirmed to interact with *FBXO2*. Purple genes are associated with ovarian cancer, blue genes are related to the immune, and green genes are linked to both ovarian cancer and the immune (Fig. 5A). The examination of the network module controlled by *FBXO2* in the KEGG analysis indicated a strong presence of the PI3K-Akt signaling pathway, focal adhesion, and ECM-receptor interaction (Fig. 5B). In addition, the results of GO functions for these genes were shown in Fig. 5C. Biologically, they were mainly enriched in extracellular matrix organization and glycoprotein metabolic process; In terms of cellular component, they were mainly enriched in endoplasmic reticulum lumen and lysosomal lumen; Regarding molecular function, enrichment was mainly observed in glycosaminoglycan binding and growth factor binding.

3.6. FBXO2 may affect tumor stemness in HGSOC

In the GSE158937 dataset, we found that *FBXO2* was highly expressed in epithelial cells and barely expressed in immune and stromal populations (Fig. 6A). KEGG analysis revealed that the DEGs in epithelial cells from two groups were predominantly enriched in oxidative phosphorylation and chemical carcinogenesis – reactive oxygen species (Fig. 6B). And the results of GO analysis for the DEGs were shown in Fig. 6C. Notably, the results of GSEA analysis suggested hypoxia pathway and interferon gamma response pathway were upregulated in the low expression group (Fig S4A-4B). Furthermore, *PEG10* was identified as the marker gene of cancer

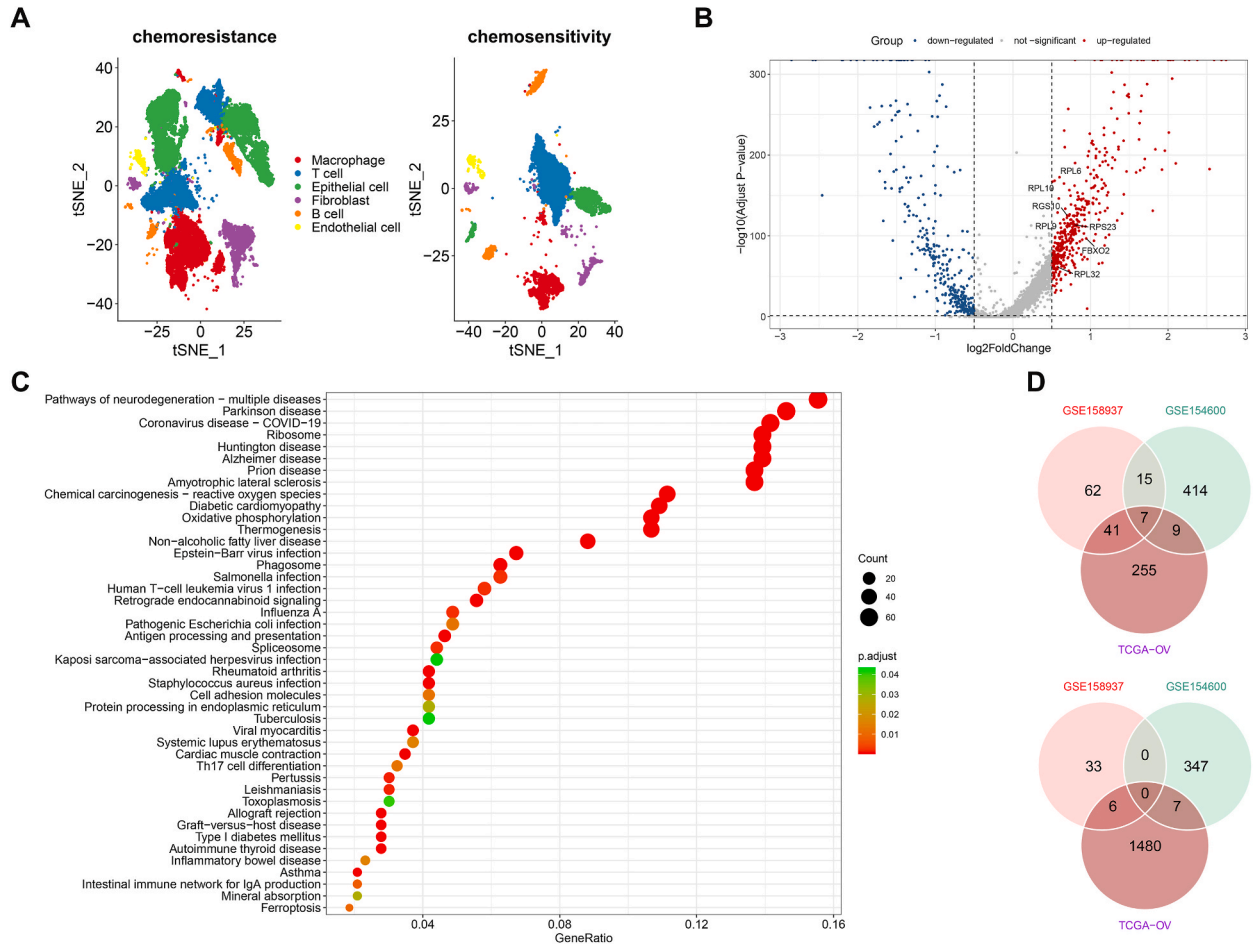

Fig. 3. Cell annotation and KEGG analysis in the GSE154600 dataset. (A) The t-SNE plot demonstrated cell types of chemoresistance samples (left) and chemosensitivity samples (right). (B) The DEGs between epithelial cells originated from chemoresistance samples and those originated from chemosensitivity samples. (C) KEGG analysis of DEGs. (D) Intersection of upregulated genes (up) and downregulated genes (down) of the GSE158937 dataset, the GSE154600 dataset and TCGA-OV dataset.

stem-like cells in HGSOC by reviewing the relevant literature [40]. As presented in Fig. 6D, there is a significant correlation between *FBXO2* expression level and *PEG10* expression level ($r = 0.25$, $P < 0.001$). It suggested that *FBXO2* may affect tumor stemness in HGSOC, which is worthy of further verification in subsequent studies.

3.7. FBXO2 silencing reduces chemoresistance

The results of Western blot experiment were shown in Fig. 7A and B and the uncropped image of Western Blot could be seen in Fig S5A-5D, which successfully confirmed the knockdown of the transcript. *FBXO2* expression was significantly higher in three ovarian cancer cell lines (A2780, OVCA429, and IGROV-1) treated with cisplatin compared to those not receiving cisplatin (Fig. 8A). In the *in vitro* experiment, the IC50 of cisplatin in the control group was 3.786 μg/ml, but the IC50 of cisplatin in the silence *FBXO2* group was 2.002 μg/ml for the A2780 human ovarian carcinoma cell line (Fig. 8B). In addition, the IC50 of cisplatin in the control group was 2.060 μg/ml; however, the IC50 of cisplatin in the silenced *FBXO2* group was 1.256 μg/ml for the SKOV3 human ovarian carcinoma cell line (Fig. 8C). These results further validated that *FBXO2* may be a potential biomarker associated with chemoresistance in HGSOC.

4. Discussions

Chemoresistance is the primary obstacle in treating patients with high-grade serous ovarian cancer [41]. Therefore, it is imperative to explore potential biomarkers that can predict the outcome of platinum chemotherapy. Fig. 9 displays the flow chart of our study. In the present study, the initial analysis of GSE158937, a single-cell RNA sequencing dataset of high-grade serous ovarian cancer, revealed that nearly all epithelial cells were cancerous Interestingly, the results of the "Scissor" algorithm showed that most cells

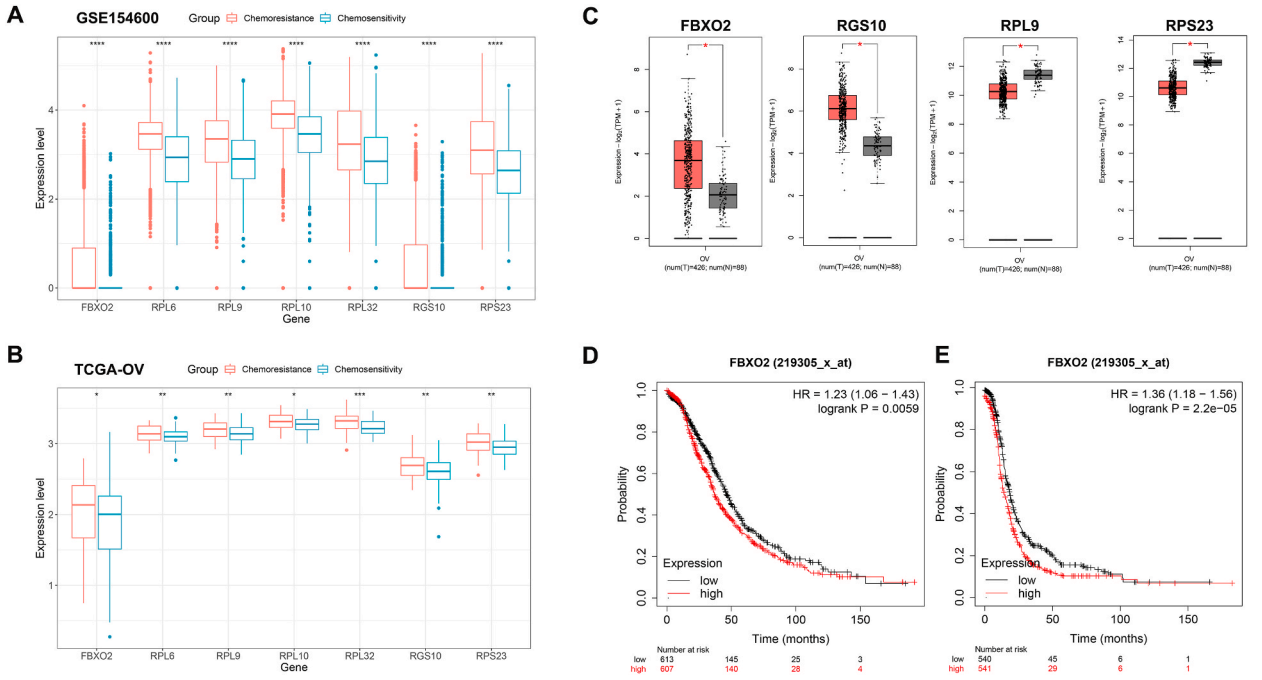

Fig. 4. Identification of candidate biomarkers. (A) The expression of overlapping genes in the GSE154600 dataset. (B) The expression of overlapping genes in TCGA-OV dataset. (C) The expression of *FBXO2*, *RGS10*, *RPL9*, and *RPS23* in tumor samples and normal samples. (D) The OS of HGSOC patients in the *FBXO2* low- and high-expression groups. (E) The PFS of HGSOC patients in the *FBXO2* low- and high-expression groups.

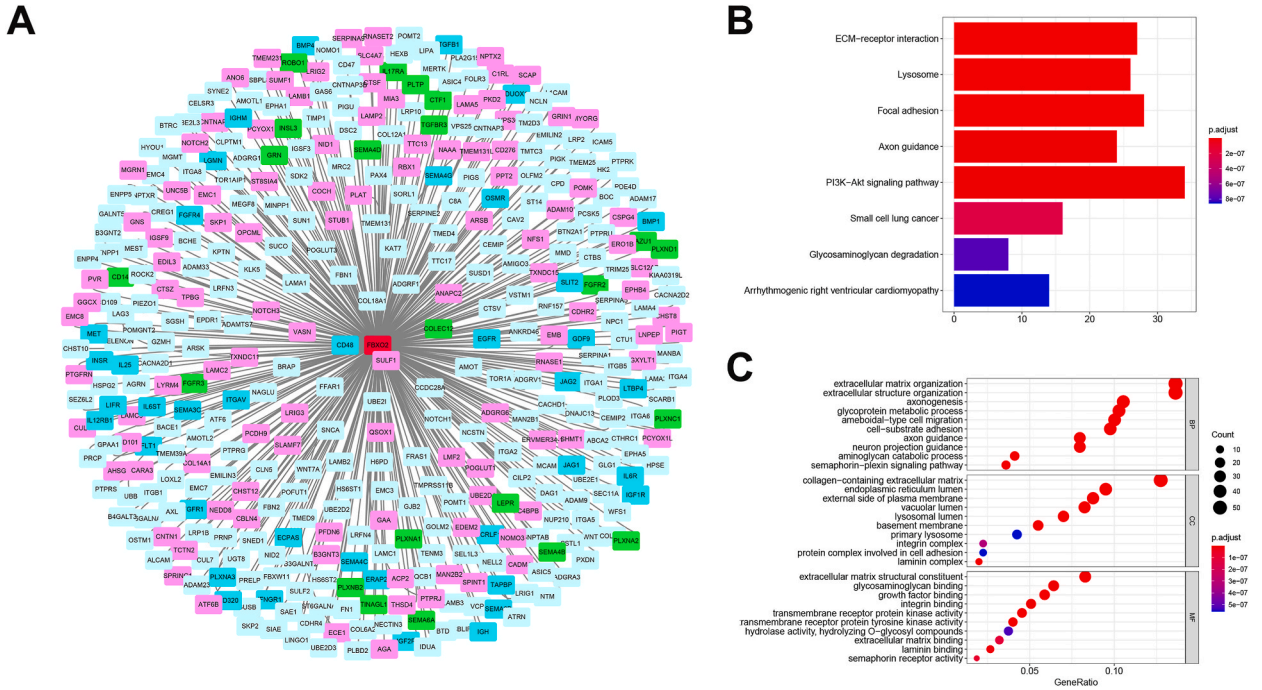

Fig. 5. PPI network and enrichment analysis of genes dominated by *FBXO2*. (A) *FBXO2*-dominated interaction network. Purple represents ovarian cancer-related genes, blue represents immune-related genes and green represents both ovarian cancer-related genes and immune-related genes. (B) KEGG analysis. (C) GO analysis.

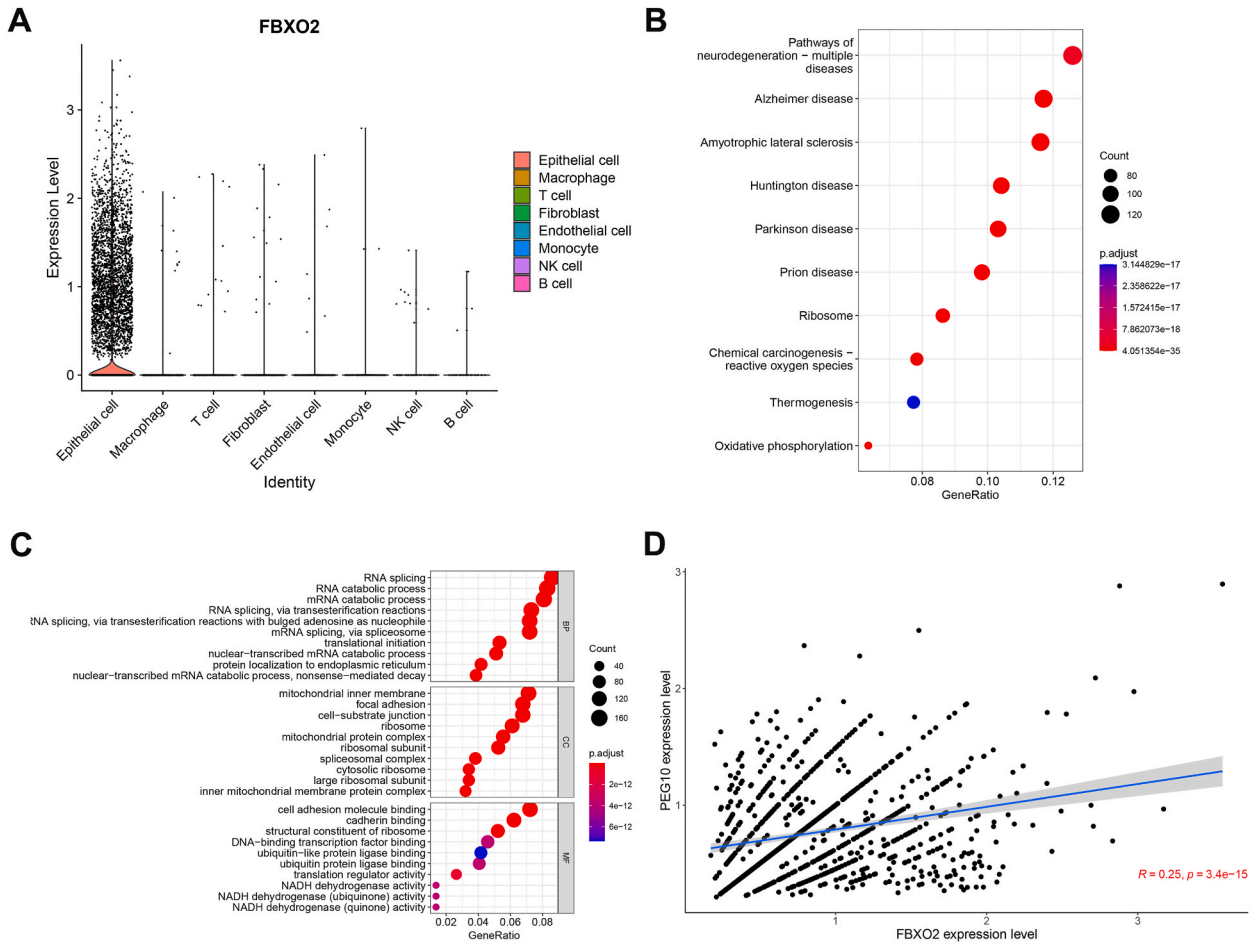

Fig. 6. Exploration of *FBXO2* expression in the GSE154600 dataset and the relationship between *FBXO2* and tumor stemness in HGSOC. (A) The expression of *FBXO2* in various cell types. (B) KEGG analysis. (C) GO analysis. (D) Correlation analysis between *FBXO2* and *PEG10*.

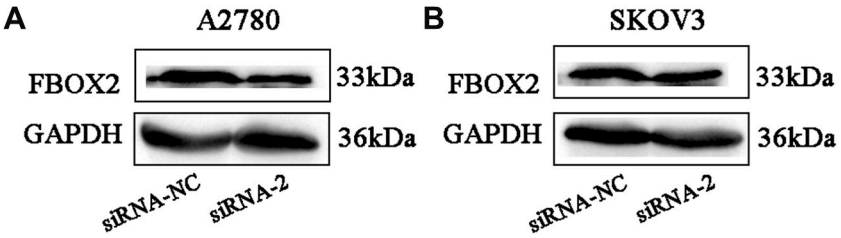

Fig. 7. Western Blot experiment. (A) The protein expression levels of *FBXO2* after knockdown in A2780 cells. (B) The protein expression levels of *FBXO2* after knockdown in SKOV3 cells.

associated with chemoresistance were epithelial cells. In fact, it has been well established that epithelial cells are the targets of chemotherapy in HGSOC [42]. To our knowledge, the "Scissor" algorithm is the first bioinformatics tool that automatically identifies the most phenotype-relevant cell subpopulations from a single-cell dataset by leveraging a bulk dataset and phenotype information. Two benefits help to enhance the overall comprehension of chemoresistance in HGSOC. A benefit of using 'Scissor' is that it eliminates the need for unsupervised clustering in single-cell data, thus preventing subjective decisions regarding cell cluster numbers or clustering resolution. Crucially, it offers a versatile structure for incorporating different external characteristics in large datasets to assist in the analysis of individual cells, allowing for the discovery of cell subgroups that are significant in both clinical and biological contexts without the need for specific hypotheses. And we believed that our results confirmed that the unique algorithm is reliable and effective again.

Revealing the potential mechanism of chemoresistance could provide great guidance to overcome the problem of chemoresistance.

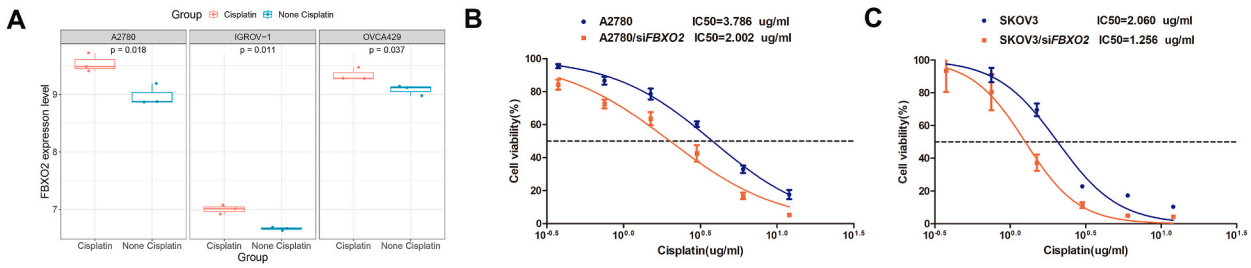

Fig. 8. Validation of *FBXO2* expression. (A) The expression level of *FBXO2* among treated with cisplatin and untreated with cisplatin group in A2780 cell line, IGROV-1 cell line and OVCA429 cell line. (B) CCK-8 assays were performed to determine the survival rates of A2780 and A2780/si*FBXO2* cells after treatment with cisplatin for 48 h. (C) CCK-8 assays were performed to determine the survival rates of SKOV3 and SKOV3/si*FBXO2* cells after treatment with cisplatin for 48 h.

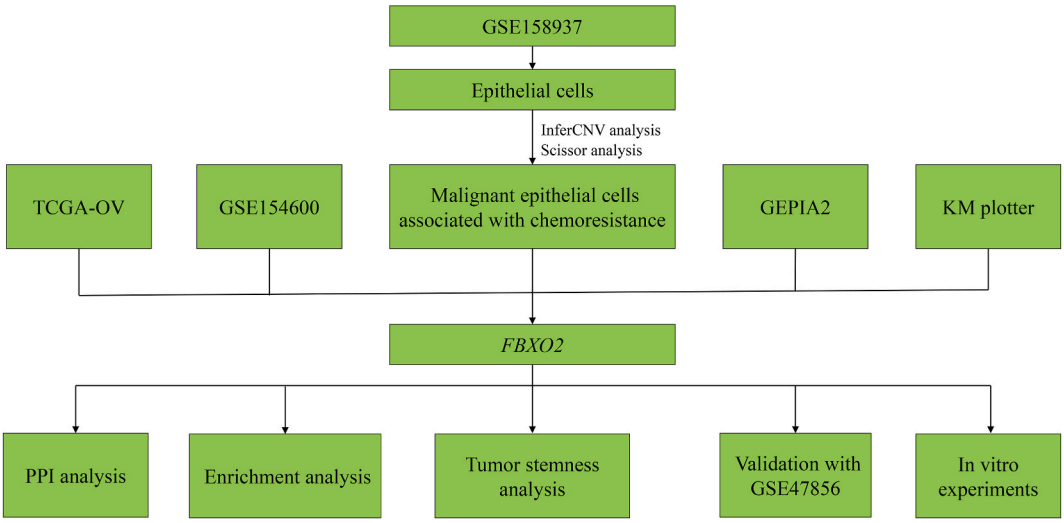

Fig. 9. The flow chart of this study.

KEGG analysis revealed that DEGs in epithelial cells related to chemoresistance were significantly enriched in ribosome, protein processing in the endoplasmic reticulum, and chemical carcinogenesis – reactive oxygen species. The significance of biosynthetic pathways in the development of chemoresistance is readily apparent. Among these pathways, *FBXO2* was enriched in protein processing in the endoplasmic reticulum. As an important organelle for protein processing, the endoplasmic reticulum is essential to maintain physiological activities. Yet, the buildup of improperly folded proteins in the endoplasmic reticulum leads to endoplasmic reticulum stress. It has been reported that endoplasmic reticulum stress has an important pathological influence on many diseases, including cancer, metabolic disorders, and neurological disorders [43–45]. Recent studies have shown a connection between endoplasmic reticulum stress and resistance to chemotherapy, with the suppression of this stress improving the efficacy of chemotherapeutics in various cancer types [46–48]. Crucially, the findings from the enrichment analysis were supported by another scRNA-seq dataset GSE154600, demonstrating the participation of epithelial cells in chemoresistance of HGSOC.

Within the GSE158937 dataset, it was observed that *FBXO2* expression was elevated in malignant epithelial cells associated with chemoresistance, as opposed to those not related to chemoresistance. Furthermore, we also found that *FBXO2* expression in epithelial cells originating from chemoresistance samples was higher than that in epithelial cells originating from chemosensitivity samples in the GSE154600 dataset. Conversely, *FBXO2* exhibited higher expression levels in tumor samples than in normal samples in the TCGA-OV dataset. To confirm whether *FBXO2* is a suitable biomarker associated with chemoresistance, the clinical value of *FBXO2* was explored. We determined that patients with high *FBXO2* expression had significantly worse OS and DFS and vice versa.

In contrast to numerous prior research efforts, our study investigated potential biomarkers linked to chemoresistance in HGSOC combining single-cell RNA-seq and bulk RNA-seq data, taking into account their individual strengths. *FBXO2*, identified as a receptor specific to glycoproteins for substrates in the SKP1/CUL1/F-box protein ubiquitin ligase complex, has been documented by numerous scientists. Che et al. reported that *FBXO2* acts as an E3 ligase that targets FBN1 for ubiquitin-dependent degradation, promoting endometrial cancer proliferation by regulating the cell cycle and the autophagy signaling pathway [49]. Sun et al. indicated that *FBXO2* enhances the proliferation and migration of human gastric cancer cells and that the expression of *FBXO2* is closely linked to lymph node metastasis [50]. Ji et al. revealed that *FBXO2* enhances the advancement of ovarian cancer by preventing cell death, and

elevated levels of *FBXO2* expression are linked to a poorer outlook [51]. Nevertheless, limited research has shown the relevance of *FBXO2* in chemoresistance in HGSOC, and our findings could offer fresh perspectives on the mechanism of chemoresistance and drug development.

In order to examine the role of *FBXO2*, we gathered genes that directly interacting with *FBXO2* and built a network module centered around *FBXO2*. From the interaction network module, we found that some genes were related to ovarian cancer and immune interactions with *FBXO2*. Various studies have demonstrated a strong connection between these genes and HGSOC. A study found that reducing *PLXNB2* levels can inhibit the proliferation and invasion of ovarian cancer cell [52]. The interaction network module suggested that *FBXO2* is crucial in the advancement and reaction to chemotherapy of HGSOC. Furthermore, the KEGG examination of the network module interaction indicated that they were mainly enriched in the PI3K-Akt signaling pathway, focal adhesion, and ECM-receptor interaction. Increasing evidence indicates that the PI3K-Akt signaling pathway plays a role in chemoresistance, with PI3K activation leading to heightened chemoresistance in cases of ovarian cancer [53–55]. Simultaneously, a clinical study showed that the combination of PI3K inhibitor alpelisib and the PARP inhibitor olaparib is viable without any unforeseen harmful impacts on individuals with epithelial ovarian cancer [56]. Additionally, a separate study demonstrated that combining the PI3K inhibitor BKM120 with olaparib can effectively treat high-grade serous ovarian carcinoma, although the dosage of BKM120 may need to be reduced [57]. Focal adhesion kinase is essential to ovarian cancer chemoresistance, and focal adhesion kinase siRNA has been demonstrated to be a novel therapeutic approach to overcome chemoresistance [58,59]. Gu et al. suggested that inhibition of the ECM-receptor interaction pathway can reduce the proliferation, migration, and invasion of ovarian cancer cells [60]. The results of our enrichment analysis indicated that *FBXO2* may affect the chemoresistance of HGSOC patients through these pathways.

Cancer stem cells, also known as CSCs, are a subset of cancer cells that have the ability to renew themselves and differentiate, supporting the growth of tumors and reproducing a diverse tumor population [61]. Accumulating evidence suggests that CSCs play a crucial role in chemoresistance in ovarian cancer. For example, Liao et al. stated that ovarian cancer stem cells have the ability to endure stressful situations, specifically low oxygen levels, and could play a role in chemoresistance [62]. In our study, we found that there is a significant correlation between *FBXO2* expression level and *PEG10* expression level. This result indicated that *FBXO2* may affect tumor stemness in HGSOC, which is worthy of further verification in subsequent studies.

Analysis of transcriptomic data of three cell lines confirmed upregulation of *FBXO2* in the group treated with cisplatin. Additionally, a test for chemosensitivity was performed to determine if reducing *FBXO2* levels would enhance the effectiveness of platinum in treating ovarian cancer. During an *in vitro* study, it was observed that the IC50 of cisplatin decreased in A2780 and SKOV3 human ovarian carcinoma cell lines when *FBXO2* was silenced, as opposed to the control group. This finding illustrated that inhibiting the expression of *FBXO2* may alleviate chemoresistance in HGSOC, which provides some guidance for clinical practice. Considering that the results of GSEA analysis suggested hypoxia pathway and interferon gamma response pathway were upregulated in the low expression group, we speculated these two pathways play a key role in alleviate chemoresistance in HGSOC when *FBXO2* is inhibited.

In conclusion, our analysis of single-cell RNA-seq and bulk RNA-seq revealed *FBXO2* as a potential biomarker linked to chemoresistance in HGSOC. The results suggest that *FBXO2* could serve as a valuable prognostic marker and potential target for drug development in the treatment of HGSOC. However, there are some limitations in our study. Firstly, tissue dissociation results in the loss of spatial information of cells, although the accuracy of identified biomarkers is enhanced by single-cell RNA sequencing; therefore, combining single-cell RNA sequencing with spatial transcriptomics may provide a more comprehensive approach. Furthermore, this study lacks experimental validation of the functional role of *FBXO2* in chemoresistance, necessitating further research to uncover it. Additionally, since our study is retrospective, it is need for future prospective, large-scale trials to substantiate the clinical applicability of our findings.

Ethics statement

Informed consent was not required for this study because no private human tissue samples or animal experiments are involved.

Consent for publication

Not applicable.

Funding

This work was supported by the National Natural Science Foundation of China (82060474 to Xiaoli Tang).

Data availability statement

The datasets were downloaded from the TCGA and GEO website and the code requests should be submitted to the corresponding author for consideration.

CRediT authorship contribution statement

Wenwen Lai: Writing – original draft, Validation, Software, Formal analysis, Conceptualization. **Ruixiang Xie:** Writing – original draft, Validation, Software, Conceptualization. **Chen Chen:** Validation, Data curation. **Weiming Lou:** Software, Formal analysis, Data

curation. **Haiyan Yang:** Validation, Data curation. **Libin Deng:** Methodology, Formal analysis. **Quqin Lu:** Methodology, Formal analysis. **Xiaoli Tang:** Writing – review & editing, Supervision, Project administration, Methodology, Funding acquisition, Conceptualization.

Declaration of competing interest

The authors declare that they have no known competing financial interests or personal relationships that could have appeared to influence the work reported in this paper.

Abbreviations

CNV	copy number variation
CSCs	Cancer stem cells
DEGs	differentially expressed genes
EOC	Epithelial ovarian cancer
FBXO2	F-box protein 2
FC	fold change
GEO	Gene Expression Omnibus
GO	Gene Ontology
GSEA	Gene set enrichment analysis
HGSOC	High-grade serous ovarian carcinoma
IC50	50% maximum inhibitory concentration
KEGG	Kyoto Encyclopedia of Genes and Genomes
OS	overall survival
PFI	platinum-free interval
PFS	progression-free survival
PPI	protein-protein interaction
RNA-seq	RNA sequencing
ScRNA-seq	single-cell RNA sequencing
TCGA-OV	The Cancer Genome Atlas-ovarian serous cystadenocarcinoma

Appendix A. Supplementary data

Supplementary data to this article can be found online at https://doi.org/10.1016/j.heliyon.2024.e28490.

References

[1] H. Sung, J. Ferlay, R.L. Siegel, M. Laversanne, I. Soerjomataram, A. Jemal, et al., Global cancer statistics 2020: GLOBOCAN estimates of incidence and mortality worldwide for 36 cancers in 185 countries, Epub 2021/02/05, CA A Cancer J. Clin. 71 (3) (2021) 209–249, https://doi.org/10.3322/caac.21660. PubMed PMID: 33538338.

[2] S. Lheureux, C. Gourley, I. Vergote, A.M. Oza, Epithelial ovarian cancer, Lancet 393 (10177) (2019) 1240–1253, https://doi.org/10.1016/s0140-6736(18)32552-2.

[3] L.A. Torre, B. Trabert, C.E. DeSantis, K.D. Miller, G. Samimi, C.D. Runowicz, et al., Ovarian cancer statistics, 2018, Epub 2018/05/29, CA A Cancer J. Clin. 68 (4) (2018) 284–296, https://doi.org/10.3322/caac.21456. PubMed PMID: 29809280; PubMed Central PMCID: PMCPMC6621554.

[4] L. Kuroki, S.R. Guntupalli, Treatment of epithelial ovarian cancer, Epub 20201109, Bmj 371 (2020) m3773, https://doi.org/10.1136/bmj.m3773. PubMed PMID: 33168565.

[5] D.D. Bowtell, S. Böhm, A.A. Ahmed, P.J. Aspuria, R.C. Bast Jr., V. Beral, et al., Rethinking ovarian cancer II: reducing mortality from high-grade serous ovarian cancer, Nat. Rev. Cancer 15 (11) (2015) 668–679, https://doi.org/10.1038/nrc4019. PubMed PMID: 26493647; PubMed Central PMCID: PMCPMC4892184.

[6] S. Pignata, C. Pisano, M. Di Napoli, S.C. Cecere, R. Tambaro, L. Attademo, Treatment of recurrent epithelial ovarian cancer, Cancer 125 (Suppl 24) (2019) 4609–4615, https://doi.org/10.1002/cncr.32500. PubMed PMID: 31967680.

[7] M. Koti, R.J. Gooding, P. Nuin, A. Haslehurst, C. Crane, J. Weberpals, et al., Identification of the IGF1/PI3K/NF κB/ERK gene signalling networks associated with chemotherapy resistance and treatment response in high-grade serous epithelial ovarian cancer, Epub 20131116, BMC Cancer 13 (2013) 549, https://doi.org/10.1186/1471-2407-13-549. PubMed PMID: 24237932; PubMed Central PMCID: PMCPMC3840597.

[8] P. Todeschini, E. Salviato, C. Romani, V. Raimondi, F. Ciccarese, F. Ferrari, et al., Comprehensive profiling of hypoxia-related miRNAs identifies miR-23a-3p overexpression as a marker of platinum resistance and poor prognosis in high-grade serous ovarian cancer, Epub 20210704, Cancers 13 (13) (2021), https://doi.org/10.3390/cancers13133358. PubMed PMID: 34283087; PubMed Central PMCID: PMCPMC8268862.

[9] Z. Liu, H. Wu, J. Deng, H. Wang, Z. Wang, A. Yang, et al., Molecular classification and immunologic characteristics of immunoreactive high-grade serous ovarian cancer, J. Cell Mol. Med. 24 (14) (2020) 8103–8114, https://doi.org/10.1111/jcmm.15441.

[10] L. Wang, F. Zhang, J.Y. Cui, L. Chen, Y.T. Chen, B.W. Liu, CAFs enhance paclitaxel resistance by inducing EMT through the IL-6/JAK2/STAT3 pathway, Epub 20180314, Oncol. Rep. 39 (5) (2018) 2081–2090, https://doi.org/10.3892/or.2018.6311. PubMed PMID: 29565447; PubMed Central PMCID: PMCPMC5928760.

[11] J. Qian, B.L. LeSavage, K.M. Hubka, C. Ma, S. Natarajan, J.T. Eggold, et al., Cancer-associated mesothelial cells promote ovarian cancer chemoresistance through paracrine osteopontin signaling, J. Clin. Invest. 131 (16) (2021), https://doi.org/10.1172/jci146186. PubMed PMID: 34396988; PubMed Central PMCID: PMCPMC8363279.

[12] H. Li, F. Luo, X. Jiang, W. Zhang, T. Xiang, Q. Pan, et al., CircITGB6 promotes ovarian cancer cisplatin resistance by resetting tumor-associated macrophage polarization toward the M2 phenotype, J Immunother Cancer 10 (3) (2022), https://doi.org/10.1136/jitc-2021-004029. PubMed PMID: 35277458; PubMed Central PMCID: PMCPMC8919471.
[13] Y. Wang, H. Xie, X. Chang, W. Hu, M. Li, Y. Li, et al., Single-cell dissection of the multiomic landscape of high-grade serous ovarian cancer, CAN-21-3819. Epub 20220815, Cancer Res. (2022), https://doi.org/10.1158/0008-5472. Can-21-3819. PubMed PMID: 35969151.
[14] B. Izar, I. Tirosh, E.H. Stover, I. Wakiro, M.S. Cuoco, I. Alter, et al., A single-cell landscape of high-grade serous ovarian cancer, Epub 20200622, Nat. Med. 26 (8) (2020) 1271–1279, https://doi.org/10.1038/s41591-020-0926-0. PubMed PMID: 32572264; PubMed Central PMCID: PMCPMC7723336.
[15] J. Xu, Y. Fang, K. Chen, S. Li, S. Tang, Y. Ren, et al., Single-cell RNA sequencing reveals the tissue architecture in human high-grade serous ovarian cancer, Clin. Cancer Res. 28 (16) (2022) 3590–3602, https://doi.org/10.1158/1078-0432.Ccr-22-0296. PubMed PMID: 35675036.
[16] K. Zhang, E.P. Erkan, S. Jamalzadeh, J. Dai, N. Andersson, K. Kaipio, et al., Longitudinal single-cell RNA-seq analysis reveals stress-promoted chemoresistance in metastatic ovarian cancer, Epub 20220223, Sci. Adv. 8 (8) (2022) eabm1831, https://doi.org/10.1126/sciadv.abm1831. PubMed PMID: 35196078; PubMed Central PMCID: PMCPMC8865800.
[17] Q. Hao, J. Li, Q. Zhang, F. Xu, B. Xie, H. Lu, et al., Single-cell transcriptomes reveal heterogeneity of high-grade serous ovarian carcinoma, Clin. Transl. Med. 11 (8) (2021) e500, https://doi.org/10.1002/ctm2.500. PubMed PMID: 34459128; PubMed Central PMCID: PMCPMC8335963.
[18] L. Liang, J. Yu, J. Li, N. Li, J. Liu, L. Xiu, et al., Integration of scRNA-seq and bulk RNA-seq to analyse the heterogeneity of ovarian cancer immune cells and establish a molecular risk model, Epub 2021/10/09, Front. Oncol. 11 (2021) 711020, https://doi.org/10.3389/fonc.2021.711020. PubMed PMID: 34621670; PubMed Central PMCID: PMCPMC8490743.
[19] Q. Tan, H. Liu, J. Xu, Y. Mo, F. Dai, Integrated analysis of tumor-associated macrophage infiltration and prognosis in ovarian cancer, Epub 2021/10/12, Aging (Albany NY) 13 (19) (2021) 23210–23232, https://doi.org/10.18632/aging.203613. PubMed PMID: 34633990; PubMed Central PMCID: PMCPMC8544311.
[20] Z. Wang, J. Zhang, F. Dai, B. Li, Y. Cheng, Integrated analysis of single-cell RNA-seq and bulk RNA-seq unveils heterogeneity and establishes a novel signature for prognosis and tumor immune microenvironment in ovarian cancer, Epub 2023/01/16, J. Ovarian Res. 16 (1) (2023) 12, https://doi.org/10.1186/s13048-022-01074-1. PubMed PMID: 36642706; PubMed Central PMCID: PMCPMC9841625.
[21] U.A. Matulonis, A.K. Sood, L. Fallowfield, B.E. Howitt, J. Sehouli, B.Y. Karlan, Ovarian cancer, Epub 20160825, Nat. Rev. Dis. Prim. 2 (2016) 16061, https://doi.org/10.1038/nrdp.2016.61. PubMed PMID: 27558151; PubMed Central PMCID: PMCPMC7290868.
[22] A.A. Hippen, M.M. Falco, L.M. Weber, E.P. Erkan, K. Zhang, J.A. Doherty, et al., miQC: an adaptive probabilistic framework for quality control of single-cell RNA-sequencing data, Epub 2021/08/25, PLoS Comput. Biol. 17 (8) (2021) e1009290, https://doi.org/10.1371/journal.pcbi.1009290. PubMed PMID: 34428202; PubMed Central PMCID: PMCPMC8415599.
[23] L.M. Weber, A.A. Hippen, P.F. Hickey, K.C. Berrett, J. Gertz, J.A. Doherty, et al., Genetic demultiplexing of pooled single-cell RNA-sequencing samples in cancer facilitates effective experimental design, Epub 2021/09/24, GigaScience 10 (9) (2021), https://doi.org/10.1093/gigascience/giab062. PubMed PMID: 34553212; PubMed Central PMCID: PMCPMC8458035.
[24] L. Geistlinger, S. Oh, M. Ramos, L. Schiffer, R.S. LaRue, C.M. Henzler, et al., Multiomic analysis of subtype evolution and heterogeneity in high-grade serous ovarian carcinoma, Epub 2020/08/05, Cancer Res. 80 (20) (2020) 4335–4345, https://doi.org/10.1158/0008-5472.Can-20-0521. PubMed PMID: 32747365; PubMed Central PMCID: PMCPMC7572645.
[25] Q.H. Miow, T.Z. Tan, J. Ye, J.A. Lau, T. Yokomizo, J.P. Thiery, et al., Epithelial-mesenchymal status renders differential responses to cisplatin in ovarian cancer, Epub 2014/05/27, Oncogene 34 (15) (2015) 1899–1907, https://doi.org/10.1038/onc.2014.136. PubMed PMID: 24858042.
[26] A. Gribov, M. Sill, S. Lück, F. Rücker, K. Döhner, L. Bullinger, et al., SEURAT: visual analytics for the integrated analysis of microarray data, Epub 20100603, BMC Med. Genom. 3 (2010) 21, https://doi.org/10.1186/1755-8794-3-21. PubMed PMID: 20525257; PubMed Central PMCID: PMCPMC2893446.
[27] M. Ringnér, What is principal component analysis? Nat. Biotechnol. 26 (3) (2008) 303–304, https://doi.org/10.1038/nbt0308-303.
[28] D. Kobak, P. Berens, The art of using t-SNE for single-cell transcriptomics, Epub 20191128, Nat. Commun. 10 (1) (2019) 5416, https://doi.org/10.1038/s41467-019-13056-x. PubMed PMID: 31780648; PubMed Central PMCID: PMCPMC6882829.
[29] D. Aran, A.P. Looney, L. Liu, E. Wu, V. Fong, A. Hsu, et al., Reference-based analysis of lung single-cell sequencing reveals a transitional profibrotic macrophage, Epub 20190114, Nat. Immunol. 20 (2) (2019) 163–172, https://doi.org/10.1038/s41590-018-0276-y. PubMed PMID: 30643263; PubMed Central PMCID: PMCPMC6340744.
[30] A.P. Patel, I. Tirosh, J.J. Trombetta, A.K. Shalek, S.M. Gillespie, H. Wakimoto, et al., Single-cell RNA-seq highlights intratumoral heterogeneity in primary glioblastoma, Epub 20140612, Science 344 (6190) (2014) 1396–1401, https://doi.org/10.1126/science.1254257. PubMed PMID: 24925914; PubMed Central PMCID: PMCPMC4123637.
[31] D. Sun, X. Guan, A.E. Moran, L.Y. Wu, D.Z. Qian, P. Schedin, et al., Identifying phenotype-associated subpopulations by integrating bulk and single-cell sequencing data, Epub 2021/11/13, Nat. Biotechnol. 40 (4) (2022) 527–538, https://doi.org/10.1038/s41587-021-01091-3. PubMed PMID: 34764492; PubMed Central PMCID: PMCPMC9010342.
[32] G. Yu, L.G. Wang, Y. Han, Q.Y. He, clusterProfiler: an R package for comparing biological themes among gene clusters, Epub 20120328, OMICS 16 (5) (2012) 284–287, https://doi.org/10.1089/omi.2011.0118. PubMed PMID: 22455463; PubMed Central PMCID: PMCPMC3339379.
[33] M.E. Ritchie, B. Phipson, D. Wu, Y. Hu, C.W. Law, W. Shi, et al., Limma powers differential expression analyses for RNA-sequencing and microarray studies, Epub 2015/01/22, Nucleic Acids Res. 43 (7) (2015) e47, https://doi.org/10.1093/nar/gkv007. PubMed PMID: 25605792; PubMed Central PMCID: PMCPMC4402510.
[34] D. Szklarczyk, A.L. Gable, K.C. Nastou, D. Lyon, R. Kirsch, S. Pyysalo, et al., The STRING database in 2021: customizable protein-protein networks, and functional characterization of user-uploaded gene/measurement sets, d12, Nucleic Acids Res. 49 (D1) (2021) D605, https://doi.org/10.1093/nar/gkaa1074. PubMed PMID: 33237311; PubMed Central PMCID: PMCPMC7779004.
[35] C. Stark, B.J. Breitkreutz, T. Reguly, L. Boucher, A. Breitkreutz, M. Tyers, BioGRID: a general repository for interaction datasets, Nucleic Acids Res. 34 (Database issue) (2006) D535–D539, https://doi.org/10.1093/nar/gkj109. PubMed PMID: 16381927; PubMed Central PMCID: PMCPMC1347471.
[36] T.S. Keshava Prasad, R. Goel, K. Kandasamy, S. Keerthikumar, S. Kumar, S. Mathivanan, et al., Human protein reference database–2009 update, Epub 20081106, Nucleic Acids Res. 37 (Database issue) (2009) D767–D772, https://doi.org/10.1093/nar/gkn892. PubMed PMID: 18988627; PubMed Central PMCID: PMCPMC2686490.
[37] C.J. Grondin, A.P. Davis, J.A. Wiegers, T.C. Wiegers, D. Sciaky, R.J. Johnson, et al., Predicting molecular mechanisms, pathways, and health outcomes induced by Juul e-cigarette aerosol chemicals using the Comparative Toxicogenomics Database, Epub 20210805, Curr Res Toxicol 2 (2021) 272–281, https://doi.org/10.1016/j.crtox.2021.08.001. PubMed PMID: 34458863; PubMed Central PMCID: PMCPMC8379377.
[38] S. Bhattacharya, P. Dunn, C.G. Thomas, B. Smith, H. Schaefer, J. Chen, et al., ImmPort, toward repurposing of open access immunological assay data for translational and clinical research, Epub 20180227, Sci. Data 5 (2018) 180015, https://doi.org/10.1038/sdata.2018.15. PubMed PMID: 29485622; PubMed Central PMCID: PMCPMC5827693.
[39] P. Shannon, A. Markiel, O. Ozier, N.S. Baliga, J.T. Wang, D. Ramage, et al., Cytoscape: a software environment for integrated models of biomolecular interaction networks, Epub 2003/11/05, Genome Res. 13 (11) (2003) 2498–2504, https://doi.org/10.1101/gr.1239303. PubMed PMID: 14597658; PubMed Central PMCID: PMCPMC403769.
[40] N. Sumitani, K. Ishida, K. Sawada, T. Kimura, Y. Kaneda, K. Nimura, Identification of malignant cell populations associated with poor prognosis in high-grade serous ovarian cancer using single-cell RNA sequencing, Epub 20220722, Cancers 14 (15) (2022), https://doi.org/10.3390/cancers14153580. PubMed PMID: 35892844; PubMed Central PMCID: PMCPMC9331511.
[41] S. Pignata, C.C. S, A. Du Bois, P. Harter, F. Heitz, Treatment of recurrent ovarian cancer, Ann. Oncol. 28 (suppl_8) (2017) viii51–v56, https://doi.org/10.1093/annonc/mdx441. PubMed PMID: 29232464.
[42] C.E. Richter, E. Cocco, S. Bellone, D.A. Silasi, D. Rüttinger, M. Azodi, et al., High-grade, chemotherapy-resistant ovarian carcinomas overexpress epithelial cell adhesion molecule (EpCAM) and are highly sensitive to immunotherapy with MT201, a fully human monoclonal anti-EpCAM antibody, Epub 20100925, Am. J.

Obstet. Gynecol. 203 (6) (2010) 582.e1–582.e7, https://doi.org/10.1016/j.ajog.2010.07.041. PubMed PMID: 20870202; PubMed Central PMCID: PMCPMC2993821.
[43] C. Li, K. Zhang, G. Pan, H. Ji, C. Li, X. Wang, et al., Dehydrodiisoeugenol inhibits colorectal cancer growth by endoplasmic reticulum stress-induced autophagic pathways, Epub 20210410, J. Exp. Clin. Cancer Res. 40 (1) (2021) 125, https://doi.org/10.1186/s13046-021-01915-9. PubMed PMID: 33838688; PubMed Central PMCID: PMCPMC8035743.
[44] X. Li, Z. Cheng, X. Chen, D. Yang, H. Li, Y. Deng, Purpurogallin improves neurological functions of cerebral ischemia and reperfusion mice by inhibiting endoplasmic reticulum stress and neuroinflammation, Epub 20220811, Int. Immunopharm. 111 (2022) 109057, https://doi.org/10.1016/j.intimp.2022.109057. PubMed PMID: 35964408.
[45] J.M. Lee, S. Park, D. Lee, R.P. Ginting, M.R. Lee, M.W. Lee, et al., Reduction in endoplasmic reticulum stress activates beige adipocytes differentiation and alleviates high fat diet-induced metabolic phenotypes, Epub 20210206, Biochim. Biophys. Acta, Mol. Basis Dis. 1867 (5) (2021) 166099, https://doi.org/10.1016/j.bbadis.2021.166099. PubMed PMID: 33556486.
[46] K.C. Huang, S.F. Chiang, P.C. Yang, T.W. Ke, T.W. Chen, C.Y. Lin, et al., ATAD3A stabilizes GRP78 to suppress ER stress for acquired chemoresistance in colorectal cancer, Epub 20210212, J. Cell. Physiol. 236 (9) (2021) 6481–6495, https://doi.org/10.1002/jcp.30323. PubMed PMID: 33580514.
[47] P.C. Thakur, J.L. Miller-Ocuin, K. Nguyen, R. Matsuda, A.D. Singhi, H.J. Zeh, et al., Inhibition of endoplasmic-reticulum-stress-mediated autophagy enhances the effectiveness of chemotherapeutics on pancreatic cancer, Epub 20180709, J. Transl. Med. 16 (1) (2018) 190, https://doi.org/10.1186/s12967-018-1562-z. PubMed PMID: 29986726; PubMed Central PMCID: PMCPMC6038181.
[48] Y. Zhu, M. Xie, Z. Meng, L.K. Leung, F.L. Chan, X. Hu, et al., Knockdown of TM9SF4 boosts ER stress to trigger cell death of chemoresistant breast cancer cells, Epub 20190627, Oncogene 38 (29) (2019) 5778–5791, https://doi.org/10.1038/s41388-019-0846-y. PubMed PMID: 31249383.
[49] X. Che, F. Jian, Y. Wang, J. Zhang, J. Shen, Q. Cheng, et al., FBXO2 promotes proliferation of endometrial cancer by ubiquitin-mediated degradation of FBN1 in the regulation of the cell cycle and the autophagy pathway, Epub 20200831, Front. Cell Dev. Biol. 8 (2020) 843, https://doi.org/10.3389/fcell.2020.00843. PubMed PMID: 32984335; PubMed Central PMCID: PMCPMC7487413.
[50] X. Sun, T. Wang, Z.R. Guan, C. Zhang, Y. Chen, J. Jin, et al., FBXO2, a novel marker for metastasis in human gastric cancer, Epub 20171218, Biochem. Biophys. Res. Commun. 495 (3) (2018) 2158–2164, https://doi.org/10.1016/j.bbrc.2017.12.097. PubMed PMID: 29269301.
[51] J. Ji, J. Shen, Y. Xu, M. Xie, Q. Qian, T. Qiu, et al., FBXO2 targets glycosylated SUN2 for ubiquitination and degradation to promote ovarian cancer development, Epub 20220507, Cell Death Dis. 13 (5) (2022) 442, https://doi.org/10.1038/s41419-022-04892-9. PubMed PMID: 35525855; PubMed Central PMCID: PMCPMC9079088.
[52] G. Xiang, Y. Cheng, MiR-126-3p inhibits ovarian cancer proliferation and invasion via targeting PLXNB2, Epub 20180724, Reprod. Biol. 18 (3) (2018) 218–224, https://doi.org/10.1016/j.repbio.2018.07.005. PubMed PMID: 30054097.
[53] Y.C. Niu, J. Tong, X.F. Shi, T. Zhang, MicroRNA-654-3p enhances cisplatin sensitivity by targeting QPRT and inhibiting the PI3K/AKT signaling pathway in ovarian cancer cells, Epub 20200611, Exp. Ther. Med. 20 (2) (2020) 1467–1479, https://doi.org/10.3892/etm.2020.8878. PubMed PMID: 32742380; PubMed Central PMCID: PMCPMC7388328.
[54] Z. Amini-Farsani, M.H. Sangtarash, M. Shamsara, H. Teimori, MiR-221/222 promote chemoresistance to cisplatin in ovarian cancer cells by targeting PTEN/PI3K/AKT signaling pathway, Epub 20170908, Cytotechnology 70 (1) (2018) 203–213, https://doi.org/10.1007/s10616-017-0134-z. PubMed PMID: 28887606; PubMed Central PMCID: PMCPMC5809651.
[55] A.M. Elsayed, E. Bayraktar, P. Amero, S.A. Salama, A.H. Abdelaziz, R.S. Ismail, et al., PRKAR1B-AS2 long noncoding RNA promotes tumorigenesis, survival, and chemoresistance via the PI3K/AKT/mTOR pathway, Epub 20210213, Int. J. Mol. Sci. 22 (4) (2021), https://doi.org/10.3390/ijms22041882. PubMed PMID: 33668685; PubMed Central PMCID: PMCPMC7918312.
[56] P.A. Konstantinopoulos, W.T. Barry, M. Birrer, S.N. Westin, K.A. Cadoo, G.I. Shapiro, et al., Olaparib and α-specific PI3K inhibitor alpelisib for patients with epithelial ovarian cancer: a dose-escalation and dose-expansion phase 1b trial, Epub 20190314, Lancet Oncol. 20 (4) (2019) 570–580, https://doi.org/10.1016/s1470-2045(18)30905-7. PubMed PMID: 30880072; PubMed Central PMCID: PMCPMC7025391.
[57] U.A. Matulonis, G.M. Wulf, W.T. Barry, M. Birrer, S.N. Westin, S. Farooq, et al., Phase I dose escalation study of the PI3kinase pathway inhibitor BKM120 and the oral poly (ADP ribose) polymerase (PARP) inhibitor olaparib for the treatment of high-grade serous ovarian and breast cancer, Ann. Oncol. 28 (3) (2017) 512–518, https://doi.org/10.1093/annonc/mdw672. PubMed PMID: 27993796; PubMed Central PMCID: PMCPMC5834157.
[58] Y. Byeon, J.W. Lee, W.S. Choi, J.E. Won, G.H. Kim, M.G. Kim, et al., CD44-Targeting PLGA nanoparticles incorporating paclitaxel and FAK siRNA overcome chemoresistance in epithelial ovarian cancer, Epub 20180816, Cancer Res. 78 (21) (2018) 6247–6256, https://doi.org/10.1158/0008-5472.Can-17-3871. PubMed PMID: 30115698.
[59] C.J. Diaz Osterman, D. Ozmadenci, E.G. Kleinschmidt, K.N. Taylor, A.M. Barrie, S. Jiang, et al., FAK activity sustains intrinsic and acquired ovarian cancer resistance to platinum chemotherapy, Epub 20190903, Elife 8 (2019) e47327, https://doi.org/10.7554/eLife.47327. PubMed PMID: 31478830; PubMed Central PMCID: PMCPMC6721800.
[60] Y. Gu, K. Huang, M. Zhang, F. Teng, L. Ge, J. Zhou, et al., Long noncoding RNA CTD-2589m5.4 inhibits ovarian cancer cell proliferation, migration, and invasion via downregulation of the extracellular matrix-receptor interaction pathway, Epub 20210708, Cancer Biother. Radiopharm. 37 (7) (2022) 580–588, https://doi.org/10.1089/cbr.2020.4429. PubMed PMID: 34242057.
[61] C.T. Jordan, M.L. Guzman, M. Noble, Cancer stem cells, N. Engl. J. Med. 355 (12) (2006) 1253–1261, https://doi.org/10.1056/NEJMra061808. PubMed PMID: 16990388.
[62] J. Liao, F. Qian, N. Tchabo, P. Mhawech-Fauceglia, A. Beck, Z. Qian, et al., Ovarian cancer spheroid cells with stem cell-like properties contribute to tumor generation, metastasis and chemotherapy resistance through hypoxia-resistant metabolism, Epub 20140107, PLoS One 9 (1) (2014) e84941, https://doi.org/10.1371/journal.pone.0084941. PubMed PMID: 24409314; PubMed Central PMCID: PMCPMC3883678.